Kinetics and Catalysis, Vol. 46, No. 6, 2005, pp. 891–899. Translated from Kinetika i Kataliz, Vol. 46, No. 6, 2005, pp. 940–948.

Effect of the Support on the Nature of Metal–Promoter Interactions in Ru–Cs^+/MgO and Ru–Cs^+–Al_2O_3 Catalysts for Ammonia Synthesis

Yu. V. Larichev*, B. L. Moroz*, E. M. Moroz*, V. I. Zaikovskii*, S. M. Yunusov, E. S. Kalyuzhnaya**, V. B. Shur**, and V. I. Bukhtiyarov***

** Boreskov Institute of Catalysis, Siberian Division, Russian Academy of Sciences, Novosibirsk, 630090 Russia*

*** Nesmeyanov Institute of Organoelement Compounds, Russian Academy of Sciences, Moscow, 119991 Russia*

Received January 26, 2005

Abstract—The Ru–Cs^+/MgO and Ru–Cs^+/γ-Al_2O_3 catalysts, which were prepared by an impregnation method using $RuOHCl_3$ and Cs_2CO_3 as precursor compounds and reduced with H_2 at 450°C, are characterized by X-ray diffraction, high-resolution transmission electron microscopy (with X-ray microanalysis), and X-ray photoelectron spectroscopy (XPS). The Cs^+/MgO(Al_2O_3) systems, Ru–Cs^+ black, and model systems prepared by cesium sputtering onto polycrystalline ruthenium foil are studied as reference samples. It is found that, in the Ru–Cs^+/MgO sample, cesium is present as a $Cs_{2+x}O$ cesium suboxide, which weakly interacts with the support, localized on the surface of Ru particles or near them. In the case of Ru–Cs^+/γ-Al_2O_3, cesium occurs as a species that is tightly bound to the support; this is likely surface cesium aluminate, which prevents promoter migration to Ru particles. The Ru–Cs^+/MgO sample exhibits a considerable shift of the Ru3*d* line in the XPS spectra toward lower binding energies, as compared to the bulk metal. It is hypothesized that this shift is due to a decrease in the electron work function from the surface of ruthenium because of the polarizing effect of Cs^+ ions in contact with Ru particles. Based on the experimental results, the great difference between the catalytic activities of the Ru–Cs^+/MgO and Ru–Cs^+/γ-Al_2O_3 systems in ammonia synthesis at 250–400°C and atmospheric pressure is explained.

INTRODUCTION

Ruthenium catalysts promoted with alkali metal compounds are highly active in ammonia synthesis at low pressures (0.1–3.0 MPa) and temperatures (250–350°C) [1]. The most active catalysts were prepared with the use of magnesium oxide as a support [2]. The replacement of MgO by alumina, a more practical substance, or various carbon materials noticeably decreased the low-temperature activity of ruthenium in the synthesis of ammonia [3, 4]. It was found that catalytic activity is related to the basicity of the support: the more basic the support, the higher the activity of the catalyst in the reaction of ammonia synthesis [4, 5]. Aika *et al.* [4] explained this correlation by electron-density transfer from the basic support (MgO) to ruthenium particles. Because of the appearance of a negative charge on metal particles, the dissociation of N_2 molecules is facilitated. This dissociation is the rate-limiting step of ammonia synthesis. This hypothesis was supported experimentally based on the decreased binding energies (E_b) of electrons in the Ru3*d* core level in Ru/MgO samples (279.2–279.5 eV), as compared with that of the bulk metal. In contrast to this, normal values of the binding energy of ruthenium metal (280.2–280.5 eV) were found in Ru/Al_2O_3(SiO_2) and Ru/C samples [4, 6, 7]. Although a negative shift of XPS spectra can in fact suggest an excessive electron density on the supported metal because of the interaction of the support with the active component, other reasons, including instrumental factors, can also be responsible for this effect. Moreover, this explanation is inconsistent with the low activity of samples based on aluminum oxide promoted with alkalis, although this modified support is highly basic [5, 8].

It is also well known that the activity of ruthenium catalysts for ammonia synthesis depends strongly on the basicity of the promoter and increases in the order Na < K < Rb < Cs [1, 9]. However, there is no direct experimental data on the electron effect of the promoter. The occurrence of an interaction between the promoter and the support and the nature of this interaction are not understood, although it is obvious that such an interaction can also affect the activity of catalysts.

The aim of this work was to study the chemical state of a promoter (a Cs^+ compound) and the interaction of this promoter with a catalytically active metal (Ru) and a support in the Ru–Cs^+/MgO and Ru–Cs^+/Al_2O_3 systems with the use of X-ray diffraction (XRD), transmission electron microscopy (TEM), and X-ray photoelectron spectroscopy (XPS).

0023-1584/05/4606-0891 © 2005 MAIK "Nauka/Interperiodica"

EXPERIMENTAL

MgO and γ-Al_2O_3 with particle sizes of 0.25–0.50 mm and specific surface areas of 200 and 220 m^2/g, respectively (determined by the low-temperature adsorption of nitrogen), were used as catalyst supports. Before sample preparation, the supports were evacuated at 450°C and 0.02 Torr for 2–3 h.

Ru/MgO and Ru/Al_2O_3 samples were prepared by the incipient wetness impregnation of the supports with a solution of $RuOHCl_3$ in acetone (of high-purity grade). Immediately after impregnation, the solvent was removed by purging the samples with air at room temperature up to a loose state. Next, the samples were evacuated at 20°C for 2 h and at 60°C for 2 h to a residual pressure of 0.02 Torr. Because of the low solubility of the ruthenium compound in acetone, the impregnation procedure was additionally performed two times. After the final cycle of impregnation, the samples were evacuated at 60°C for 6 h and then reduced in a flow of H_2 (80 ml/min) in a glass tube reactor. The reactor temperature was increased stepwise to 450°C for 2–2.5 h; next, the samples were reduced for 6 h at this temperature. After the reduction, the samples were cooled to room temperature in a flow of H_2, removed from the reactor, and kept under argon.

The cesium promoter was introduced in accordance with a published procedure [5], which was modified. A weighed portion of Cs_2CO_3 was dissolved in absolute ethanol at 70°C, and the solution was added to a reduced Ru/MgO or Ru/Al_2O_3 sample thermostated at the specified temperature (the solution volume added was approximately equal to the pore volume of the support). The solvent was distilled off in a flow of argon, and the sample was evacuated at 20°C for 2 h and at 60°C for 2 h to a residual pressure of 0.02 Torr. Because Cs_2CO_3 is sparingly soluble in absolute ethanol even on heating, the impregnation procedure was additionally repeated three times. After the completion of impregnation, the samples were evacuated at 60°C for 6 h and treated with hydrogen. The procedure and conditions of hydrogen treatment were analogous to those described above.

According to X-ray fluorescence analysis data, the concentrations of ruthenium and cesium in Ru–Cs^+/MgO and Ru–Cs^+/Al_2O_3 samples were the same and equal to 4.5 and 4.0 wt % for Ru and Cs, respectively (the Cs : Ru atomic ratio was 0.8).

The reference samples of Cs^+/MgO and Cs^+/Al_2O_3 were prepared in accordance with a procedure analogous to that described above for the introduction of a cesium promoter into Ru/MgO and Ru/Al_2O_3 samples. According to X-ray fluorescence analysis data, the concentrations of cesium in the Cs^+/MgO and Cs^+/Al_2O_3 samples were 3.5 and 4.8 wt %, respectively.

Ruthenium black promoted with Cs^+ ions was prepared as described below. The reduction of $RuOHCl_3$ with formaldehyde in an aqueous alkali solution at 80°C [10] afforded ruthenium black, which was washed with distilled water and dried. Thereafter, an aqueous solution of cesium carbonate, which was taken in a fourfold excess by volume with respect to black, was added. The mixture was evaporated to dryness at 50°C with continuous stirring. The dry residue was evacuated at 20°C for 2 h and at 60°C for 6 h to a residual pressure of 0.02 Torr and treated with hydrogen under conditions analogous to those described above. The resulting sample contained three weight parts of Ru and one weight part of Cs.

The catalytic activity of Ru/MgO and Ru–Cs^+/MgO samples in ammonia synthesis was studied in a glass fixed-bed flow reactor at 200–400°C and atmospheric pressure with the use of a stoichiometric mixture of $N_2 + H_2$ (the rate of gas supply to the reactor was 10 l/h). The gas mixture was purified in order to remove trace oxygen, moisture, and other impurities. A weighed portion of a catalyst was placed in the reactor away from air in a flow of the $N_2 + H_2$ mixture and heated to a specified temperature. The ammonia content of a gas flow at the reactor outlet was determined by measuring changes in the concentration of a dilute aqueous H_2SO_4 solution through which the gas was passed. Tests at the specified temperature were continued until the catalyst reached a steady state; thereafter, the reaction temperature was increased by 50°C and the steady-state concentration of NH_3 in the reactor outlet gas was determined once again (the steady-state concentration of NH_3 was calculated by averaging the results of 6–10 measurements at a constant temperature).

High-resolution TEM micrographs were obtained on a JEM-2010 instrument with a maximum grid resolution of 0.14 nm and an accelerating voltage of 200 kV. The sample was removed from an ampule filled with argon immediately before taking the micrographs, rapidly ground in air, and suspended in hexane. A drop of the suspension was applied to a porous carbon film fixed on copper gauze; thereafter, the solvent was allowed to evaporate. To obtain the particle-size distribution of Ru (TEM bar graphs) and to determine the statistically valid average particle size for each particular sample, the linear dimensions of no less than 300 particles were measured. The elemental composition of particles visible to the microscope was determined by energy dispersive X-ray (EDX) analysis using an EDAX energy dispersive spectrometer with an Si(Li) detector with a resolution of 130 eV.

The XRD analysis of samples was performed on an HZG-4 X-ray diffractometer (CuK_α radiation with a diffracted beam graphite monochromator) with a scan step of 0.05°. The size of the coherent-scattering regions of ruthenium particles was determined from the broadening of diffraction peaks and calculated with consideration for the instrumental line width using the Selyakov–Scherrer formula. Before recording XRD patterns, the sample was rapidly ground in air and wrapped in an organic polymer film to protect the sam-

ple from contact with air in the course of measurements.

The XPS spectra were measured on a VG ESCALAB HP electron spectrometer using unmonochromatized AlK_α radiation ($E_{h\nu}$ = 1486.6 eV; power of 200 W). The scale of binding energies (E_b) was precalibrated with reference to the peak positions of Au Au $4f_{7/2}$ (84.0 eV) and Cu $2p_{3/2}$ (932.6 eV) core levels from polycrystalline gold and copper foils, respectively. We used the internal standard method for the correct calibration of photoelectron lines, in particular, for the elimination of a charging effect, which occurs in a study of nonconducting samples. The Mg 2*s* line with E_b = 88.1 eV and the Al 2*p* line with E_b = 74.5 eV served as internal standards for samples containing MgO and Al_2O_3, respectively. The value of charging was determined as the difference between the measured and tabulated values of E_b; the XPS lines of the other elements were then shifted by this value. The ratios between the surface atomic concentrations of elements in the samples were determined from the integrated intensities of XPS lines corrected for corresponding atomic sensitivity factors [11]. Before measuring the spectra, the samples of supported systems were pressed into nickel gauze and placed in the preparation chamber of the spectrometer (in the course of this procedure, the samples were in air for no longer than 5 min). In the spectrometer, the samples were additionally treated with hydrogen under static conditions at 350°C and a pressure of 0.1 MPa for 1 h. The samples containing a thin film of CsO_x on the surface of polycrystalline ruthenium were prepared immediately in the preparation chamber of the XPS spectrometer either in a vacuum ($<5 \times 10^{-7}$ Pa) or in flowing oxygen (1×10^{-2} Pa).

RESULTS

The catalytic activity of Ru–Cs^+/MgO and Ru–Cs^+/Al_2O_3 samples was tested in ammonia synthesis at 200–400°C and an atmospheric pressure of the 1 : 3 mixture of N_2 and H_2. Table 1 summarizes the steady-state concentrations of NH_3 in a gas flow at the reactor outlet, which were measured in the presence of the Ru–Cs^+/MgO catalyst at various temperatures. The formation of NH_3 on this catalyst was observed from 250°C; the concentrations of NH_3 in the gas at 350 and 400°C were 79 and 100% of an equilibrium concentration, respectively. In the presence of the Ru–Cs^+/Al_2O_3 sample, the concentration of NH_3 in the exit gas was below the determination limit (<0.005 vol %) throughout temperature range examined.

Table 2 summarizes the average linear ($\langle d_l \rangle$) and volume–surface ($\langle d_{vs} \rangle$) particle sizes of ruthenium in Ru–Cs^+/MgO and Ru–Cs^+/Al_2O_3 samples and Ru–Cs^+ black, as calculated from TEM bar graphs. In the supported systems, the major amount of ruthenium particles was small ($\langle d_l \rangle$ ~2–3 nm); the fractions of coarser particles (of size 5–12 nm), which can also be seen in TEM micrographs, were approximately equal ($\langle d_{vs} \rangle$ = 9.5 and 8.3 nm for Ru–Cs^+/MgO and Ru–Cs^+/Al_2O_3, respectively). Ruthenium black promoted with a cesium compound consisted of much coarser particles about several tens of nanometers in size.

Table 1. Results of the catalytic tests of Ru–Cs^+/MgO in ammonia synthesis

Temperature, °C	$[NH_3]_{eq}$, vol %	$[NH_3]_{st}$, vol %
250	5.40	0.014
300	2.17	0.15
350	0.86	0.67
400	0.44	0.43

Note: $[NH_3]_{eq}$ is the equilibrium concentration according to published data [12]; $[NH_3]_{st}$ is the steady-state concentration in a gas at the reactor outlet. Atmospheric pressure; H_2/N_2 = 3 : 1; catalyst weight, 3.39 g.

Table 2. Ruthenium particle sizes in supported Ru–Cs^+ systems and Ru–Cs^+ black according to TEM and XRD data

Sample	$\langle d \rangle$, nm	d_{vs}, nm	Coherent-scattering region, nm
Ru–Cs^+/MgO	3.0	9.5	9.0
Ru–Cs^+/Al_2O_3	2.1	8.3	4.0
Ru–Cs^+ black	36	63	47

Figure 1 shows the high-resolution TEM images of Ru–Cs^+/MgO and Ru–Cs^+/Al_2O_3 samples. Periodicity, which corresponds to Ru–Ru interplanar spacing (d_{100} = 0.234 nm, d_{101} = 0.206 nm, etc.), can be clearly seen in ruthenium metal particles. A thin layer of a disordered structure <1 nm in thickness was detected on ruthenium metal particles in the Ru–Cs^+/MgO sample (Fig. 1a). This layer was also present on the surface of MgO but only in a narrow region (5–10 nm in diameter) near a metal particle. At the same time, the presence of this layer on the metal and support surfaces was not detected in the Ru–Cs^+/Al_2O_3 sample (Fig. 1b). Figure 2 demonstrates the EDX spectra of surface regions adjacent to ruthenium particles in Ru–Cs^+/MgO and Ru–Cs^+/Al_2O_3 samples. The spectrum of the Ru–Cs^+/MgO sample exhibited a maximum due to cesium along with the signal of ruthenium, whereas a signal of cesium was not detected in the Ru–Cs^+/Al_2O_3 sample. An analogous pattern was observed in many surface regions of the test samples. This result allowed us to assume that, in the Ru–Cs^+/MgO sample, the layer that covers ruthenium particles and the support surface near these particles contained cesium.

The XRD patterns from the supported systems exhibited only reflections due to ruthenium metal and the corresponding support (MgO or Al_2O_3). Table 2 summarizes the sizes of the coherent-scattering regions of ruthenium particles in the Ru–Cs^+/MgO and Ru–Cs^+/Al_2O_3 samples and Ru–Cs^+ black. The size of the coherent-scattering region found for the Ru–Cs^+/MgO sample is consistent with the value of $\langle d_{vs} \rangle$ for ruthenium particles

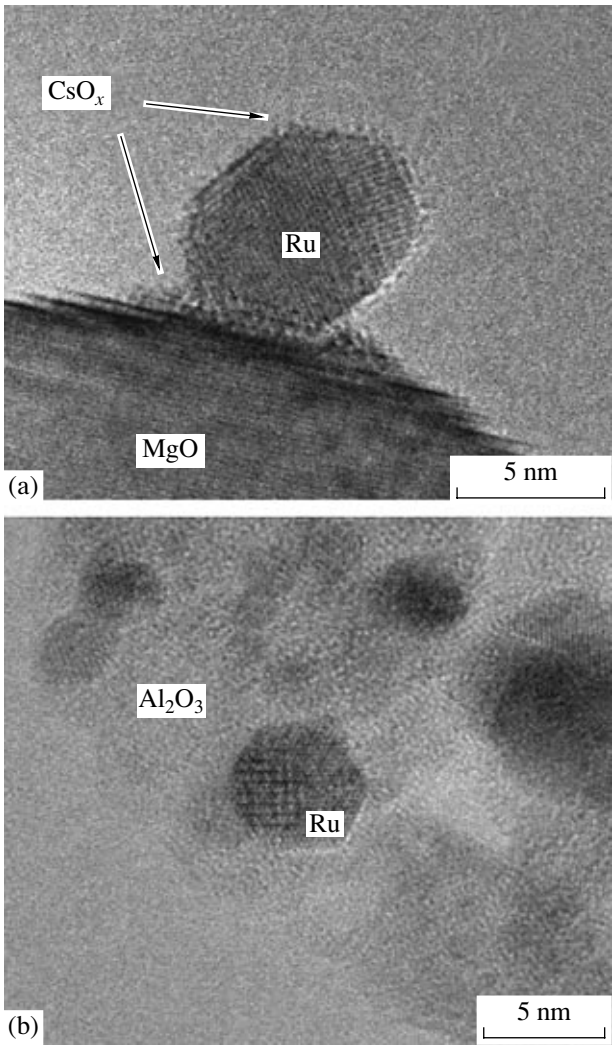

Fig. 1. Electron micrographs of the surfaces of (a) Ru–Cs^+/MgO and (b) Ru–Cs^+/Al_2O_3 samples. Magnification of 800000.

found from TEM data. The Ru–Cs^+/Al_2O_3 sample exhibited a considerable discrepancy between the values of the coherent-scattering regions and $\langle d_{vs} \rangle$, which may be due to a great number of defects in ruthenium particles.

Figure 3 compares the XRD patterns from the Ru–Cs^+/Al_2O_3 sample and the original support. The supported system exhibited an increase in the signal intensity at $2\theta = 25°–40°$, as compared with Al_2O_3. This is also characteristic of Cs^+/Al_2O_3. It is believed that this change was due to the presence of X-ray amorphous cesium compounds in the Ru–Cs^+/Al_2O_3 and Cs^+/Al_2O_3 samples. In particular, the reflections of the cesium aluminate $Cs_2Al_2O_4$ [JCPDS No. 23-0882] were observed in this region of 2θ.

Figure 4 shows the XRD pattern of a freshly reduced sample of Ru–Cs^+ black. Although the cesium content of this sample was high (25 wt %), the diffraction pattern exhibited only a weak broadened maximum at 14.5°, which can correspond to the group of reflections due to the stoichiometric cesium suboxide Cs_4O [JCPDS No. 28-0327]. After keeping the sample in air for two weeks, a group of reflections related to cesium hydrocarbonate $CsHCO_3$ [JCPDS No. 26-0376] appeared in the diffraction pattern. It is likely that cesium occurred as a thin film of cesium suboxide in the initial sample; in contact with air, this cesium suboxide was converted into the hydrocarbonate.

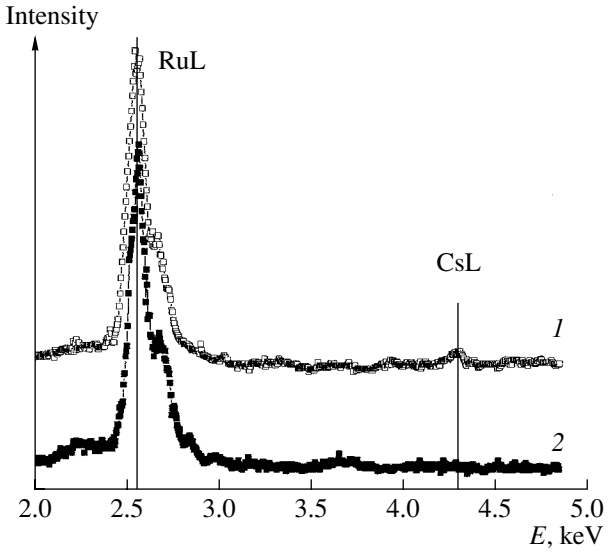

Fig. 2. Secondary X-ray (EDX) spectra from (*1*) Ru–Cs^+/MgO and (*2*) Ru–Cs^+/Al_2O_3 sample surface regions adjacent to ruthenium particles, which are shown in Fig. 1.

Figure 5 shows the Ru 3*d* XPS spectra of the supported samples after treatment with hydrogen. The values of Ru $3d_{5/2}$ E_b for Ru–Cs^+/MgO, Ru–Cs^+/Al_2O_3, and Ru–Cs^+ black are equal to 279.0, 280.2, and 280.1 eV, respectively. The value of Ru $3d_{5/2}$ E_b for the Ru–Cs^+/MgO sample is lower than the value of Ru $3d_{5/2}$ E_b measured in polycrystalline ruthenium foil (280.2 eV) by 1.2 eV. Previously, Muhler *et al.* [5] observed a shift of lines in the Ru $3d_{5/2}$ spectra of Ru/MgO systems toward lower values of E_b with reference to the corresponding line in the spectrum of bulk ruthenium and interpreted this shift as a result of electron-density transfer from the support to supported ruthenium particles.

However, note that the shift of an XPS line toward lower E_b with reference to the line of bulk metal can result from not only the appearance of a negative charge on the atoms of supported metal particles but also the occurrence of a relaxation effect and differential charging, which can occur in systems that consist of phases with different conductions (in our case, support and metal phases) [13–15]. We calculated corrections to the values of Ru $3d_{5/2}$ E_b in accordance with a published procedure [13, 15] in order to take into account relaxation and differential charging effects. With consider-

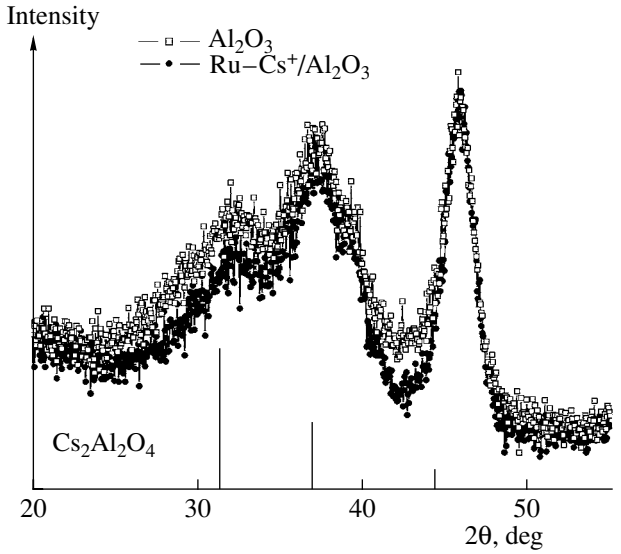

Fig. 3. Diffraction patterns of the γ-Al_2O_3 support and the Ru–Cs^+/Al_2O_3 catalyst.

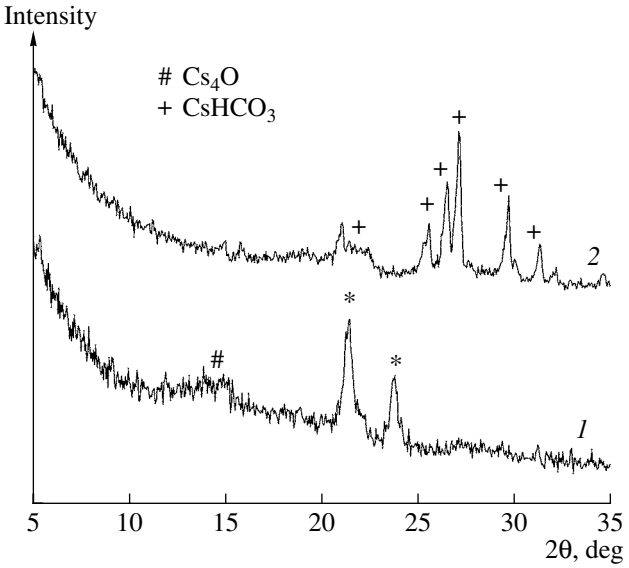

Fig. 4. Diffraction patterns of Ru–Cs^+ black (*1*) after reduction with hydrogen at 450°C and (*2*) after keeping in air for two weeks. Reflections due to an organic polymer film in which the reduced sample was wrapped to protect it from oxidation with air are marked with asterisks.

ation for these corrections, the values of Ru $3d_{5/2}$ E_b for the Ru–Cs^+/MgO and Cs^+/Al_2O_3 samples are 279.7 and 280.6 eV, respectively. Thus, even with consideration for the relaxation and differential charging effects, the value of Ru $3d_{5/2}$ E_b in the Ru $3d$ spectrum of the Ru–Cs^+/MgO sample remained lower than that in the spectrum of the bulk metal (ΔE_b = –0.5 eV).

Figure 6 shows the Cs $3d_{5/2}$ spectra measured in Ru–Cs^+/MgO and Cs^+/Al_2O_3 samples both immediately after loading into the photoelectron spectrometer in air and after treatment with hydrogen in the spectrometer. Table 3 summarizes the values of Cs $3d_{5/2}$ E_b for various cesium compounds with oxygen. These values, which were taken from [16–18], can be used for the assignment of the values of E_b in the experimental spectra. Lines in the Cs $3d_{5/2}$ spectra measured after exposure of the samples to air exhibited maximums at 724.8 and 724.9 eV for Ru–Cs^+/MgO and Ru–Cs^+/Al_2O_3, respectively. These values of Cs $3d_{5/2}$ E_b lie between the values found for the individual compounds Cs_2O_2 (E_b = 724.5 eV) and Cs_2O (E_b = 725.2 eV). Because it is well known [16, 17] that the cesium oxide Cs_2O is easily converted into the peroxide Cs_2O_2 even in the presence of trace oxygen at a very short exposure (>(5–10) × 10^{-6} Torr s), it is believed that cesium occurred as peroxide in the tested samples at least after keeping the samples in air. The treatment of the Ru–Cs^+/MgO sample with hydrogen in the spectrometer chamber at 350°C and 0.1 MPa resulted in a shift of the line maximum to E_b = 725.5 eV. Because cesium and some other metals (such as Ag, Cd, and Ba) exhibited inverse chemical shifts when the value of E_b increased rather than decreased as the oxidation state of metal decreased (see Table 3), we can state that the observed shift of the Cs $3d_{5/2}$ line toward higher values of E_b was due to the reduction of Cs^+ ions with the formation of a cesium suboxide like $Cs_{2+x}O$. The treatment of the Ru–Cs^+/Al_2O_3 sample with hydrogen under the same conditions did not cause changes in the spectrum.

The values of E_b for Cs^+/MgO and Cs^+/Al_2O_3 samples after contact with air were found to equal 724.9 and 725.1 eV, respectively. These values remained practically unchanged after the treatment of the sam-

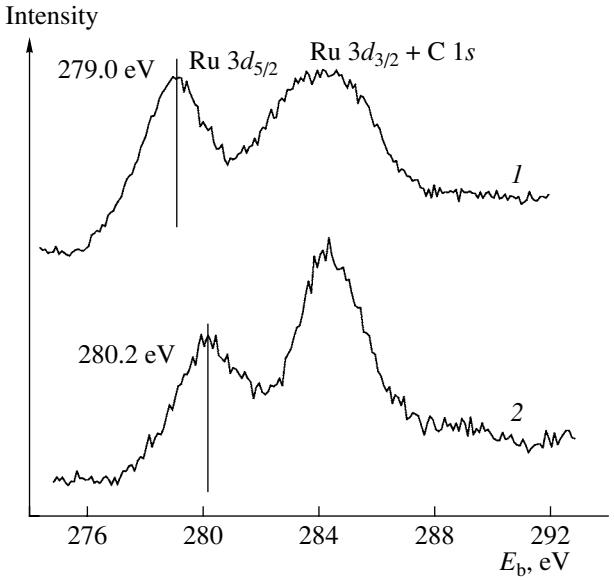

Fig. 5. Ru $3d_{5/2}$ spectra of (*1*) Ru–Cs^+/MgO and (*2*) Ru–Cs^+/Al_2O_3 samples after hydrogen treatment within the spectrometer. The spectra include a C 1s line at 285.0 eV from carbon impurities.

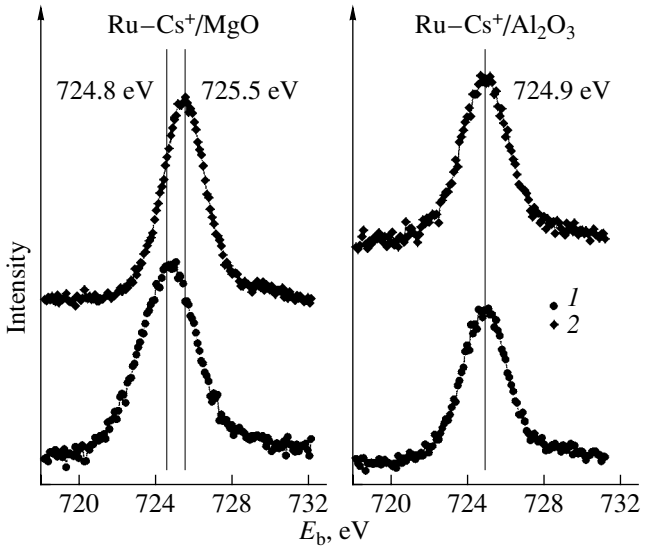

Fig. 6. Cs $3d_{5/2}$ spectra of Ru–Cs^+/MgO and Ru–Cs^+/Al_2O_3 samples (*1*) before and (*2*) after hydrogen treatment within the spectrometer.

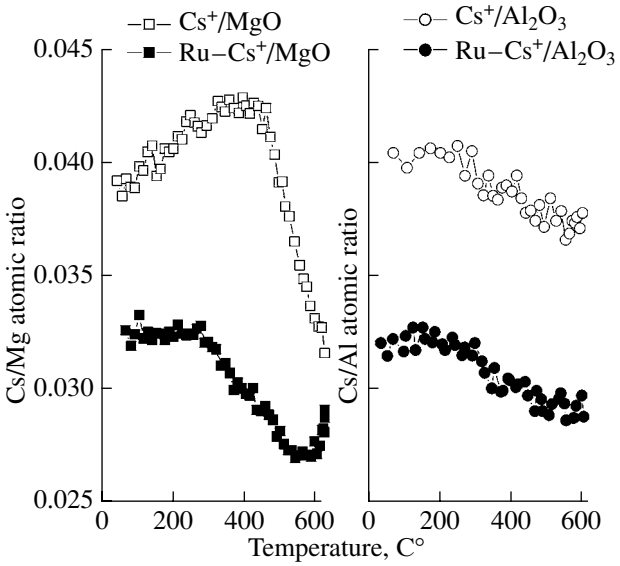

Fig. 7. The temperature dependence of surface Cs/Mg(Al) atomic ratios in Ru–Cs^+/MgO(Al_2O_3) and Cs^+/MgO(Al_2O_3) samples.

ples with hydrogen in the spectrometer chamber (E_b = 725.0 and 725.1 eV, respectively).

The line maximum in the Cs $3d_{5/2}$ spectrum of Ru–Cs^+ black measured after exposure of the sample to air was observed at E_b = 725.0 eV; after the treatment of the sample with hydrogen in the spectrometer, the line shifted to 725.5 eV. Thus, after both oxidative and reductive treatments, the chemical state of cesium in Ru–Cs^+ black was analogous to the state of cesium in the Ru–Cs^+/MgO sample after corresponding treatments.

Figure 7 illustrates the results of experiments in the course of which the Cs $3d_{5/2}$ and Mg 2*s* (or Al 2*s*) spectra of Ru–Cs^+/MgO(Al_2O_3) and Cs^+/MgO(Al_2O_3) samples were measured as the temperature was increased from room temperature to 620°C at a constant rate of 0.2 K/s. The Cs/Mg(Al) atomic ratios depending on temperature were determined from the experimental spectra. Figure 7 shows that, in all cases, the values of Cs/Mg(Al) changed only slightly with temperature at $T \le 300$°C. As the temperature was further increased, the Ru–Cs^+/MgO and Cs^+/MgO samples exhibited a considerable decrease in the Cs/Mg ratio, whereas the Cs/Al ratio also changed only slightly with temperature in the case of Ru–Cs^+/Al_2O_3 and Ru–Al_2O_3. The experimental data can be qualitatively interpreted so that the cesium promoter possessed certain mobility on the surface of MgO, whereas this mobility was not observed in the systems based on Al_2O_3; it is believed that, in this case, the promoter is strongly bound to the support surface.

Table 3. Cs $3d_{5/2}$ and O 1*s* binding energies (E_b) for various cesium compounds

Compound	E_b, eV	
	Cs $3d_{5/2}$	O 1*s*
Cs_{metal}	726.1	–
$Cs_{2+x}O$	725.5	531.0
Cs_2O	725.0	528.2
Cs_2O_2	724.5	530.6
Cs_2O_4	724.2	532.9
CsOH	724.1	–

Table 4 summarizes the values of Cs $3d_{5/2}$ and O 1*s* E_b and the surface Cs/O atomic ratios for samples prepared by cesium sputtering onto the surface of polycrystalline ruthenium foil in a vacuum or in a flow of oxygen. In this case, the values of O 1*s* E_b, which are characteristic of various cesium compounds with oxygen, can be used for the identification of surface compounds in addition to the values of Cs $3d_{5/2}$ E_b. A comparison of the values of O 1*s* E_b obtained in this work with published data [16–18], which are given in Table 3, allowed us to conclude that, upon vacuum sputtering, the surface of ruthenium foil was covered with a layer of cesium suboxide $Cs_{2+x}O$, which was formed by the interaction of cesium metal vapor with trace oxygen in the spectrometer chamber. Cesium peroxide Cs_2O_2 was formed upon cesium sputtering in a flow of O_2. The fact that the surface Cs/O atomic ratio found for ruthenium foil coated with a layer of $Cs_{2+x}O$ was lower than 2 (Cs/O = 1.9) can be due to the partial oxidation of cesium suboxide with trace oxygen that was present in the spectrometer chamber. In the case of ruthenium foil coated with a layer of Cs_2O, the deviation of the Cs/O ratio from a stoichiometric value (Cs/O = 0.89 in place of 1) can be explained by the formation of an amount of the superoxide Cs_2O_4. The O 1*s*

Table 4. Cs $3d_{5/2}$ and O 1*s* binding energies (E_b) and ratios between the surface atomic concentrations of cesium and oxygen for model systems prepared by cesium sputtering onto the surface of polycrystalline ruthenium foil

Sputtering procedure	E_b, eV		Cs/O	Assignment
	Cs $3d_{5/2}$	O 1*s*		
In a vacuum ($<5 \times 10^{-7}$ Pa)	725.8	531.5	1.90	$Cs_{2+x}O$/Ru
In a flow of O_2 (1×10^{-2} Pa)	725.0	530.5	0.89	Cs_2O_2/Ru

spectrum of the Cs_2O_2/Ru-foil sample exhibited a component with E_b = 533.5 eV, which is usually attributed to Cs_2O_4 [18], in addition to the main signal at E_b = 530.5 eV.

Thus, the results of an XPS study of model samples containing films of a cesium compound with oxygen on the surface of polycrystalline ruthenium foil demonstrated that Cs $3d_{5/2}$ lines in the range E_b = 725.4–725.8 eV, which were observed in the spectra of reduced supported Ru–Cs^+ systems and Ru–Cs^+ black, can be attributed to cesium suboxide $Cs_{2+x}O$ (although the partial presence of Cs_2O also cannot be excluded in this case), whereas Cs $3d_{5/2}$ lines in the range E_b = 724.7–725.2 eV, which were observed in the spectra of the above samples after oxidation in air, belong to cesium peroxide Cs_2O_2.

DISCUSSION

In this study, the test materials were the Ru–Cs^+/MgO and Ru–Cs^+/Al_2O_3 systems prepared by the same procedure (sequential impregnation of the support with nonaqueous solutions of $RuOHCl_3$ and Cs_2CO_3 with the high-temperature treatment of the supported compounds with hydrogen) with approximately equal concentrations of Ru and Cs. However, these systems demonstrated dramatically different catalytic activities toward ammonia synthesis: the Ru–Cs^+/MgO catalyst exhibited noticeable activity in this reaction from 250°C and a near-equilibrium yield of NH_3 was reached on this catalyst at 350°C (Table 1), whereas the formation of detectable amounts of NH_3 in the presence of Ru–Cs^+/Al_2O_3 was not observed even at 400°C.

According to XRD and TEM data, the particle-size distributions and average particle sizes of ruthenium in the Ru–Cs^+/MgO and Ru–Cs^+/Al_2O_3 samples were approximately the same (Table 2). Therefore, in this case, the difference in catalytic activity cannot be explained by a different dispersity of ruthenium.

At the same time, XPS data exhibited a difference in the electronic states of ruthenium in the Ru–Cs^+/MgO and Ru–Cs^+/Al_2O_3 samples; in both cases, the electronic state of ruthenium was different from the electronic state of Ru atoms in bulk metal. The Ru $3d_{5/2}$ line observed in the spectrum of the Ru–Cs^+/MgO sample was shifted toward lower values of E_b by 1.2 eV with reference to the spectrum of polycrystalline ruthenium foil (Fig. 5). An analogous negative shift of the Ru 3*d* spectrum, as compared with the spectrum of bulk ruthenium metal, was found previously [15] in a sample of Ru/MgO free of an alkaline promoter. In this case, it was found that this shift was only due to the effect of differential charging of the sample surface because of different conductivities of MgO and supported ruthenium metal phases. In the case of Ru–Cs^+/MgO, after taking into account the effect of differential charging and the effect of relaxation [13], the negative shift of the Ru $3d_{5/2}$ line with reference to the corresponding line in the spectrum of bulk metal was retained, although the value of this shift somewhat decreased (ΔE_b = –0.5 eV). This result suggests that electron density on ruthenium particles in the Ru–Cs^+/MgO system was in reality increased primarily because of the interaction of ruthenium with the cesium promoter rather than the support.

A hypothesis on the chemical state of cesium in the Ru–Cs^+/MgO catalyst can be proposed based on the values of Cs $3d_{5/2}$ E_b observed in the XPS spectrum of this sample after treatments with air and hydrogen (Fig. 5). To attribute these values to particular states of cesium, we used both published data (Table 3) and XPS data in the Cs $3d_{5/2}$ and O 1*s* regions for model samples prepared by cesium sputtering onto polycrystalline ruthenium foil (Table 4). An analysis of this set of data allowed us to conclude that the promoter mainly occurred as cesium suboxide $Cs_{2+x}O$ in the Ru–Cs^+/MgO sample after its high-temperature treatment with hydrogen. In contact with the sample with oxygen, $Cs_{2+x}O$ was converted into cesium peroxide Cs_2O_2, which can be reduced with hydrogen once again to $Cs_{2+x}O$. Because the XRD pattern of the Ru–Cs^+/MgO catalyst exhibited no reflections due to $Cs_{2+x}O$ and/or Cs_2O_2 phases (Fig. 3) and the high-resolution TEM images exhibited no bulk structures other than ruthenium particles and the support, we can hypothesize that the promoter in this sample did not form a crystallized phase but occurred only as a surface compound. Note that, according to XPS data, the alkali metal also occurred in the ionic form in the Cs^+/MgO reference sample after its contact with air. However, hydrogen treatment at 350°C and 0.1 MPa did not result in the formation of cesium suboxide in this case. It is likely that the presence of ruthenium metal as an activator of molecular hydrogen is necessary for this; after the dissociative chemisorption of H_2 molecules on ruthenium, hydrogen atoms are transferred to Cs^+ ions in one way or another to reduce them.

High-resolution TEM data obtained with the use of EDX indicate that ruthenium particles in the Ru–Cs^+/MgO

sample were coated with a layer containing cesium (Figs. 1a, 2). With consideration for the above XPS data, it is reasonable to assume that this layer in reduced or oxidized samples was surface cesium suboxide $Cs_{2+x}O$ or cesium peroxide Cs_2O_2, respectively. The same layer covered MgO surface regions adjacent to ruthenium particles; however, it was invisible in MgO surface regions free of ruthenium particles. This observation indicates that, in the Ru–Cs^+/MgO sample, the promoter was primarily localized on the surface of ruthenium particles and tightly bound to them. The migration of a promoter layer to the support can occur only within the limits of small MgO surface regions adjacent to ruthenium particles. Previously, in a study of model systems prepared by cesium sputtering onto a single crystal of silver metal and Ag–Cs^+/Al_2O_3 catalysts, it was found that the film of cesium suboxide can be fixed on the surface of silver by the formation of Ag–Cs bonds [19]. It is reasonable to assume that such an interaction between the cesium promoter and the transition metal (Ru) also takes place in the Ru–Cs^+/MgO system.

Various mechanisms of the effect of a cesium layer that covers ruthenium particles on the electronic state of these particles can be conceived. Only one of them, electron-density transfer from the alkaline promoter to ruthenium particles, has usually been considered for Ru–Cs^+/MgO systems [4, 5]. The experimental data on the chemical state of the promoter cast doubt on the possibility of this transfer because the promoter is a cesium compound with oxygen rather than cesium metal. An alternative mechanism implies that cesium ions on the surface of ruthenium particles exert a polarizing effect, which decreases the work function of electrons from the surface of ruthenium. An effect of this kind has long been found in many systems of bulk transition metals surface-coated with films of alkali metal compounds (for example, cesium–silver S1 photocathodes) [18]. It is clear that, in the case of supported systems where the support is a dielectric (such as MgO or Al_2O_3) and, consequently, there is no electric contact between the Fermi levels of the spectrometer and the supported metal, a decrease in the work function of electrons results in a shift of the metal line in the XPS spectrum toward lower values of E_b. In contrast, in the case of bulk systems where contact between the Fermi levels of the spectrometer and the metal is retained, a change in the work function does not cause a line shift in the XPS spectrum. Indeed, a negative shift of the Ru $3d_{5/2}$ line similar to that observed in the Ru–Cs^+/MgO sample was absent from the spectrum of Ru–Cs^+ black, although it is likely that direct contact between ruthenium metal and a cesium compound occurred in this black.

The high-resolution TEM micrographs of the Ru–Cs^+/Al_2O_3 sample did not exhibit a coating of ruthenium particles with a layer of any compound (Fig. 1b). It follows from the Cs $3d_{5/2}$ spectra that cesium occurred as a Cs^+ compound in the sample and this compound was not reduced upon hydrogen treatment in the spectrometer chamber (Fig. 6). A negative line shift with reference to the corresponding signal in the spectrum of bulk ruthenium was absent from the Ru $3d$ spectrum. The value of Ru $3d_{5/2}$ E_b for Ru–Cs^+/Al_2O_3 with consideration for differential charging and relaxation effects was 280.6 eV (Fig. 5), which is typical of ruthenium on oxide supports. On this basis, we can conclude that, in this case, the presence of cesium did not cause a decrease in the work function of electrons from the surface of ruthenium, most likely, because of the absence of contact between the cesium compound and the surface of ruthenium particles.

The question arises, why did the coating of ruthenium particles with a film of cesium suboxide occur with the use of MgO as a support and not occur in the case of Al_2O_3? This question can be tackled based on an analysis of the temperature dependence of surface Cs/Mg(Al) atomic concentration ratios in the test systems (Fig. 7). In the Ru–Cs^+/MgO and Cs^+/MgO systems, heating at $T > 300$°C significantly changed the surface concentration of cesium, whereas the surface concentration of cesium depended on temperature only slightly over the entire range of test temperatures in the case of analogous systems based on Al_2O_3. This result suggests that surface cesium suboxide in the Ru–Cs^+/MgO sample possessed certain mobility, whereas cesium was strongly bound to the support in the systems based on Al_2O_3. The XRD data (Fig. 3) allowed us to assume that, in these systems, cesium occurred as the surface cesium aluminate $Cs_2Al_2O_4$, which resulted from the reaction of Cs_2CO_3 with Al_2O_3; this reaction can occur under conditions of the hydrogen treatment of samples at 450°C. It is well known that alkali metal aluminates are refractory and that they cannot possess surface mobility at the temperatures of XPS measurements ($T \le 600$°C). In contrast to amphoteric Al_2O_3, magnesium oxide is a typical base and it can hardly react with cesium carbonate or cesium oxides, which are strong bases. Consequently, cesium suboxide can migrate over the surface of MgO and come into contact with ruthenium particles to facilitate a decrease in the work function of electrons from the surface of ruthenium. In the case of Al_2O_3, the initial promoter species is bound to oxygen centers to lose the capacity for interaction with ruthenium particles.

In accordance with the current concepts of the mechanism of ammonia synthesis on ruthenium catalysts [1, 4, 5], the work function of electrons from the surface of ruthenium has a significant effect on catalytic activity. A decrease in the work function facilitates electron transfer from the surface of ruthenium to the antibonding molecular orbital of the adsorbed N_2 molecule and thereby facilitates N_2 dissociation, which is the most difficult step of ammonia synthesis. Hence, it is believed that the contact of ruthenium particles with a film of cesium suboxide, which results in a decrease in the work function of electrons, is of importance for the Ru–Cs^+/support system to exhibit considerable cat-

alytic activity toward ammonia synthesis. This can explain the fact that the Ru–Cs^+/MgO catalyst, in which this contact takes place, exhibits activity in ammonia synthesis, whereas an analogous system based on Al_2O_3, in which there is no contact of this kind because of the interaction of the promoter with the support, was found to be inactive in this reaction.

The above assumptions also explain the well-known fact that Ru–Cs^+/Al_2O_3 systems can exhibit catalytic activity in ammonia synthesis but only at a very high promoter concentration (Cs/Ru atomic ratio ≥ 3.0) [3, 8]. It is likely that, at a high promoter concentration, a portion of the promoter remains unbound to Al_2O_3 and enters into contact with ruthenium particles.

ACKNOWLEDGMENTS

This work was supported by the Russian Foundation for Basic Research (project no. 02-03-32681). Yu.V. Larichev acknowledges the support of the Zamaraev International Charity Scientific Foundation.

REFERENCES

1. Anastasiadi, S.A., Semenova, T.A., Rabina, P.D., and Kuznetsov, L.D., *Nizkotempraturnyi ruteniisoderzhashchii katalizator sinteza ammiaka: obzornaya informatsiya* (Low-Temperature Ruthenium-Containing Catalyst for Ammonia Synthesis: A Review), *Prom–st Proizvod. Miner. Udobr., Ser.: Azotn. Prom–st*, Moscow: NIITEKhIM, 1988.
2. Moggi, P., Predieri, G., and Maione, A., *Catal. Lett.*, 2002, vol. 79, p. 7.
3. Rosowski, F., Hornung, A., Hinrichsen, O., Herein, D., Muhler, M., and Ertl, G., *Appl. Catal., A*, 1997, vol. 151, p. 443.
4. Aika, K., Shimazaki, K., Hattori, Y., Ohya, A., Ohshima, S., Shirota, K., and Ozaki, A., *J. Catal.*, 1985, vol. 92, p. 305.
5. Muhler, M., Rosowski, F., Hinrichsen, O., Hornung, A., and Ertl, G., *Stud. Surf. Sci. Catal.*, 1996, vol. 101, p. 317.
6. Larichev, Yu.V., Prosvirin, I.P., Shlyapin, D.A., Shitova, N.B., Tsyrul'nikov, P.G., and Bukhtiyarov, V.I., *Kinet. Katal.*, 2005, vol. 46, no. 4, p. 635.
7. Cattania, M.G., Parmigiani, F., and Ragani, V., *Surf. Sci.*, 1989, vols. 211/212, p. 1097.
8. Moggi, P., Albanesi, G., Predieri, G., and Spoto, G., *Appl. Catal., A*, 1995, vol. 123, p. 145.
9. Hikita, T., Aika, K., and Onishi, T., *Catal. Lett.*, 1990, vol. 4, p. 157.
10. Kobayashi, M. and Shirasaki, T., *J. Catal.*, 1973, vol. 28, p. 289.
11. *Practical Surface Analysis by Auger and X-ray Photoelectron Spectroscopy*, Briggs, D. and Seah, M., Eds., Chichester: Wiley, 1983.
12. Kuznetsov, L.D., Dmitrenko, L.D., Rabina, P.D., and Sokolinskii, Yu.A., *Sintez ammiaka* (Ammonia Synthesis), Moscow: Khimiya, 1982.
13. Bukhtiyarov, V.I., Prosvirin, I.P., and Kvon, R.I., *J. Electron Spectrosc. Relat. Phenom.*, 1996, vol. 77, p. 7.
14. Barr, T.L., *Crit. Rev. Anal. Chem.*, 1991, vol. 22, p. 229.
15. Larichev, Y.V., Moroz, B.L., Prosvirin, I.P., Bukhtiyarov, V.I., and Likholobov, V.A., *Chem. Sustainable Dev.*, 2003, vol. 11, p. 155.
16. Hwang, C.C., An, K.S., Park, R.J, Kim, J.S., Lee, J.B., Park, C.Y., Lee, S.B., Kimura, A., and Kakizaki, A, *J. Electron Spectrosc. Relat. Phenom.*, 1998, vol. 88, p. 733.
17. Ebbinghaus, G. and Simon, A., *Chem. Phys.*, 1997, vol. 43, p. 117.
18. Yang, S.J. and Bates, C.W., *Appl. Phys. Lett.*, 1980, vol. 36, p. 675.
19. Podgornov, E.A., Prosvirin, I.P., and Bukhtiyarov, V.I., *J. Mol. Catal. A*, 2000, vol. 158, p. 337.